analytical chemistry

ARTICLE

pubs.acs.org/ac

Optimization of Phosphatase- and Redox Cycling-Based Immunosensors and Its Application to Ultrasensitive Detection of Troponin I

Md. Rajibul Akanda,[†] Md. Abdul Aziz,[†] Kyungmin Jo,[†] Vellaiappillai Tamilavan,[†] Myung Ho Hyun,[†] Sinyoung Kim,[‡] and Haesik Yang*[,†]

[†]Department of Chemistry and Chemistry Institute for Functional Materials, Pusan National University, Busan 609-735, Korea

[‡]Department of Laboratory Medicine, Yonsei University College of Medicine, Seoul 135-720, Korea

Supporting Information

ABSTRACT: The authors herein report optimized conditions for ultrasensitive phosphatase-based immunosensors (using redox cycling by a reducing agent) that can be simply prepared and readily applied to microfabricated electrodes. The optimized conditions were applied to the ultrasensitive detection of cardiac troponin I in human serum. The preparation of an immunosensing layer was based on passive adsorption of avidin (in carbonate buffer (pH 9.6)) onto indium−tin oxide (ITO) electrodes. The immunosensing layer allows very low levels of nonspecific binding of proteins. The optimum conditions for the enzymatic reaction were investigated in terms of the type of buffer solution, temperature, and concentration of $MgCl_2$, and the optimum conditions for antigen−antibody binding were determined in terms of incubation time, temperature, and concentration of phosphatase-conjugated IgG. Very importantly, the antigen−antibody binding at 4 °C is extremely important in obtaining reproducible results. Among the four phosphatase substrates (L-ascorbic acid 2-phosphate (AAP), 4-aminophenyl phosphate, 1-naphthyl phosphate, 4-amino-1-naphthyl phosphate) and four phosphatase products (L-ascorbic acid (AA), 4-aminophenol, 1-naphthol, 4-amino-1-naphthol), AAP and AA meet the requirements most for obtaining easy dissolution and high signal-to-background ratios. More importantly, fast AA electrooxidation at the ITO electrodes does not require modification with any electrocatalyst or electron mediator. Furthermore, tris(2-carboxyethyl)phosphine (TCEP) as a reducing agent allows fast redox cycling, along with very low anodic currents at the ITO electrodes. Under these optimized conditions, the detection limit of an immunosensor for troponin I obtained without redox cycling of AA by TCEP is ca. 100 fg/mL, and with redox cycling it is ca. 10 fg/mL. A detection limit of 10 fg/mL was also obtained even when an immunosensing layer was simply formed on a micropatterned ITO electrode. From a practical point of view, it is of great importance that ultralow detection limits can be obtained with simply prepared enzyme-based immunosensors.

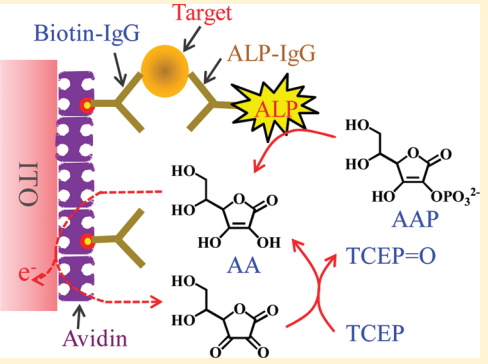

Acute myocardial infarction has been one of the leading causes of death in the world.[1−3] Rapid identification and diagnosis of acute myocardial infarction is critical for the initiation of effective medical treatment and management. Cardiac troponins are sensitive and specific biomarkers of myocardial damage; they can also be used for therapeutic monitoring and risk stratification of the disease.[1−3] However, the major limitation in currently used cardiac troponin assays is low sensitivity and precision at the time of a patient's presentation, owing to a delayed increase in circulating levels of cardiac troponin. This calls for a highly sensitive and reproducible method for detecting cardiac troponins.

Alkaline phosphatase (ALP) is a common enzyme label for signal amplification in immunoassays;[4−6] it allows a steady reaction rate for a prolonged time and shows long-term stability even in nonsterile environments.[7] In particular, ALP can generate electroactive products by enzymatic hydrolysis of substrates, and additional signal amplification by redox cycling of the products can offer higher electrochemical signals.[4,8−10] Moreover, electrochemical immunosensors can be readily miniaturized. For these reasons, many ALP-based electrochemical immunosensors have been developed, with one in particular being commercialized for point-of-care testing of cardiac biomarkers.[1] In recent years, ALP-based electrochemical immunosensors have been considered important for the development of point-of-care testing systems.[1,11,12] The authors have reported that redox cycling can be obtained in a simple one-electrode, one-enzyme format without the need to use two working electrodes or two enzymes and that indium−tin oxide (ITO) electrodes offer low

Received: February 28, 2011
Accepted: April 12, 2011
Published: April 12, 2011

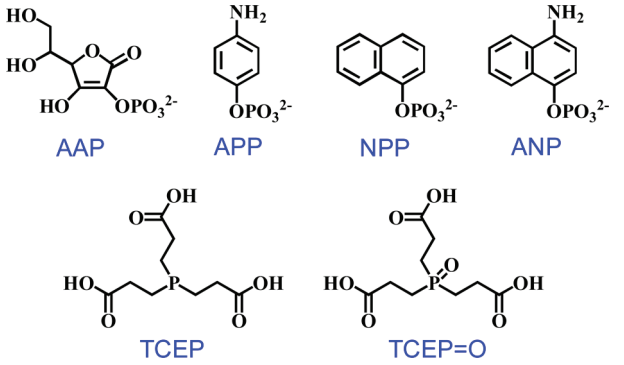

Figure 1. Chemical structures of ALP substrates and TCEP.

and reproducible background current levels.[4] However, the strong reducing agent (hydrazine) used for the chemical redox cycling is unsuitable for point-of-care testing systems because hydrazine reacts slowly with oxygen; furthermore, the preparation of the immunosensing surface is very complicated.

Several phosphates (Figure 1) have been developed as ALP substrates for electrochemical immunosensors.[13] In order to obtain a high signal-to-background ratio, an ALP substrate should be electrochemically inactive, whereas the electrochemical oxidation of the ALP product should occur both at a low formal potential and at a high reaction rate.[4] In particular, to achieve a high single-to-background ratio via redox cycling by a reducing agent, the low formal potential of the ALP product is of great importance because the unwanted oxidation currents of the reducing agent increase with increase of the applied potential. 4-Aminophenyl phosphate (APP) is the most commonly used ALP substrate.[4,6,12,13] However, it is relatively unstable in an aqueous solution[14] and the electrooxidation of its ALP product, 4-aminophenol (AP), is slow at ITO electrodes, which requires modification of an electrode with an electron-mediating material such as ferrocene.[4,15] Moreover, special care is required for rapid dissolution of AP and APP in aqueous solutions. L-Ascorbic acid 2-phosphate (AAP), used widely as a skin whitener and radical scavenger in cosmetic products, is highly water-soluble, stable, and inexpensive.[13,16−18] Furthermore, the formal potential of AA is very low. However, AAP has never been used in ITO-based electrochemical immunosensors.

Tris(2-carboxyethyl)phosphine (TCEP) is a commonly employed reducing agent for breaking disulfide bonds.[19] TCEP can reduce electroactive organic materials such as dehydroascorbic acid[20] and quinone[21] at a fast rate. Moreover, it is highly water-soluble, stable in a wide range of pHs, and quite resistant to oxidation by oxygen.[19] Its hydrochloride salt is also stable in air and nonvolatile.[19] These characteristics of TCEP are well-suited to the conditions required for prolonged storage.

Ultrasensitive detection cannot be obtained without ensuring high reproducibility of sensor signals, although high signal amplification and low background level are met. In general, reaction temperature, nonspecific binding, and complexity of sensor fabrication influence sensor signals. Antigen−antibody bindings and enzymatic reactions are highly dependent upon temperature. Nonspecific binding of proteins causes poor reproducibility of signals as well as a high background level.[22] As for sensor fabrication, a complex preparation procedure of an immunosensing surface impairs reproducibility. Accordingly, it is essential to achieve optimum control of temperature, a low level of nonspecific binding, and a simple preparation of an immunosensing surface.

Herein, the authors report optimized conditions for ultrasensitive ALP-based immunosensors using redox cycling by a reducing agent. To compare AAP with other ALP substrates and AA with other ALP products in terms of achieving an ultralow detection limit, electrochemical behaviors of four ALP substrates and their ALP products were examined in the absence and presence of TCEP. The optimum conditions for enzymatic reaction and antigen−antibody binding were then investigated. The level of nonspecific binding to avidin and bovine serum albumin (BSA) modified ITO electrodes was also investigated. Under optimized conditions, detection limits for mouse IgG and troponin I were determined in the absence and presence of the redox cycling. The same experiments were carried out with an immunosensor for troponin I using a micropatterned immunosensing layer.

EXPERIMENTAL SECTION

Materials. Avidin, biotin, 4-hydroxyazobenzene-2-carboxylic acid (HABA), biotinylated polyclonal goat antimouse IgG, mouse IgG, and ALP-conjugated polyclonal goat antimouse IgG were obtained from Sigma-Aldrich, Co. Cardiac troponin I (30R-AT035), biotinylated monoclonal mouse antitroponin-I IgG (61R-T123GBT), troponin-I-free human serum (90R-106X), and monoclonal mouse antitroponin-I IgG (10R-T123B) were obtained from Fitzerald, Inc. (Acton, MA, U.S.A.). The ALP labeling kit (LK59-10) was purchased from Dojindo Laboratories (Rockville, MD, U.S.A.). ALP-conjugated antitroponin-I IgG was prepared using antitroponin-I IgG and the ALP labeling kit according to the manufacturer's procedure. TCEP hydrochloride, AP, 1-naphthol (NP), 1-naphthyl phosphate (NPP) disodium salt, AA, 4-amino-1-naphthol (AN), and 4-nitrophenyl phosphate were obtained from Sigma-Aldrich Co. AAP magnesium salt hydrate was obtained from Wako Pure Chemical Industries, Ltd. (Osaka, Japan), while APP monosodium salt hydrate was obtained from Biosynth (Staad, Switzerland). 4-Amino-1-naphthyl phosphate (ANP) was synthesized by following a reported procedure.[23] All other reagents were received from Sigma-Aldrich Co.

The phosphate-buffered saline (PBS buffer, pH 7.4) contained 10 mM phosphate, 0.138 M NaCl, and 2.7 mM KCl. The PBSB buffer contained all of the ingredients of the PBS buffer plus 1% (w/v) BSA. The rinsing buffer (pH 7.6) contained 50 mM tris(hydroxymethyl)aminomethane (Tris), 40 mM HCl, 0.05% (w/v) BSA, and 0.5 M NaCl. The Tris-buffered saline (TBS buffer, pH 8) contained 50 mM Tris, 0.138 M NaCl, and 2.7 mM KCl. The Tris buffer (pH 9.6) for enzymatic reaction contained 50 mM Tris and 10 mM $MgCl_2$, with the pH adjusted by adding 1.0 M HCl dropwise. All ITO electrodes were obtained from Samsung Corning (Daegu, Korea). ITO micropatterns on a glass substrate were fabricated via standard photolithography and etching processes as previously reported.[24]

Preparation of Immunosensing Layers and the Immunosensing Procedure. Diced ITO electrodes (1 cm × 2 cm each) were cleaned and pretreated as reported previously.[4] To obtain avidin-and-BSA-modified ITO electrodes, the ITO electrodes were treated with avidin and subsequently BSA. To immobilize biotinylated IgG on avidin, the modified electrodes were treated with biotinylated antitroponin-I IgG (or biotinylated antimouse IgG). For the binding of target protein to the immunosensing electrodes, the immunosensing electrodes were treated with different concentrations of troponin I (or different concentrations

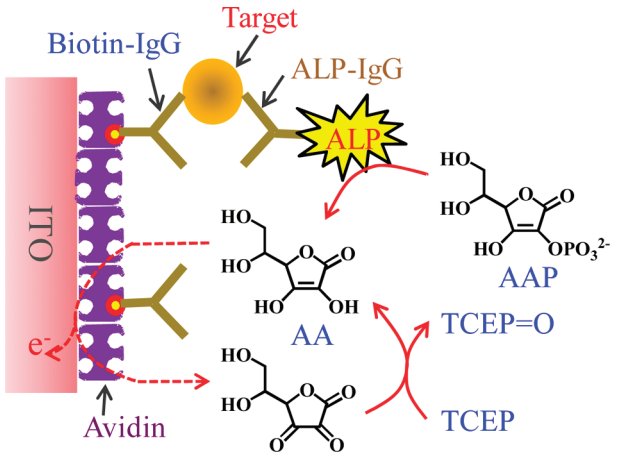

Figure 2. Schematic representation of an electrochemical immunosensor using the generation of AA by ALP and the redox cycling of AA by TCEP.

of mouse IgG). Afterward, the resulting electrodes were treated with ALP-conjugated antitroponin-I IgG (or ALP-conjugated antimouse IgG). The same procedure was used for preparation of the immunosensing layers on micropatterned ITO electrodes and for immunosensing with them. More detailed procedures are shown in the Supporting Information. For the preparation of ITO electrodes modified with ALP-conjugated antimouse IgG, 70 μL of a PBSB buffer solution (pH 7.4) containing 100 μg/mL ALP-conjugated antimouse IgG was dropped onto the pretreated ITO electrodes, the dropped state was maintained for 2 h, and the electrodes were washed twice with rinsing buffer.

Teflon electrochemical cells were assembled with the resulting electrodes, and 1.5 mL of a Tris buffer solution containing ALP substrate (and TCEP) was injected into the cell. The exposed area of the sensing electrodes was 0.28 cm^2. Afterward, the cell was stored for 10 min at 30 °C for the enzymatic reaction, and the electrochemical measurement was then carried out using a CHI 405A or CHI 708C (CH Instruments, Austin, TX, U.S.A.). The electrochemical cell included a Pt counter electrode and a Ag/AgCl reference electrode.

The experimental procedure for measuring the surface concentration of avidin is shown in the Supporting Information.

RESULTS AND DISCUSSION

Comparison of AAP with Other ALP Substrates. The schematic diagram of an electrochemical immunosensor shown in Figure 2 is based on electrochemical detection using an enzymatic reaction and a redox cycling by a reducing agent.[4] ALP products other than AA can also be utilized in the redox cycling by TCEP. To compare (i) AAP with other ALP substrates and (ii) AA with other ALP products in terms of achieving an ultralow detection limit, we investigated the electrochemical behavior of four ALP substrates (AAP, APP, NPP, ANP) and their ALP products (AA, AP, NP, AN) in the absence and presence of TCEP. The ALP substrates and products are depicted in Figure 1.

Generally, low electrocatalytic activities of ITO electrodes allow one to obtain low, flat, and reproducible capacitive currents and low electrooxidation rates for strong reducing agents.[4,25] These characteristics are effective for obtaining low background levels. However, the low activities of the ITO electrodes can cause low electrooxidation rates for ALP products, which is not good for obtaining high signal levels. Therefore, it is of great importance to select an ALP product that shows a high electrooxidation rate even at immunosensing-layer-modified ITO electrodes.

Electrochemical signals depend on the formal potential of an electroactive species and its electron-transfer rate at an electrode. In order to achieve a high signal-to-background ratio, the ALP substrate, product, and reducing agent need to meet the following requirements: (i) the ALP substrate should have a high formal potential and/or a low electrooxidation rate at the ITO electrodes; (ii) the ALP product should have a low formal potential and a high electrooxidation rate; (iii) the reducing agent should have a low electrooxidation rate and a formal potential lower than that of the ALP product. It is important to note that the ALP product should have a low formal potential (near 0 V) because unwanted anodic current of the reducing agent is higher at higher potentials and unwanted cathodic current of oxygen is considerable at potentials lower than 0 V.

Curves i of Figure 3 represent cyclic voltammograms obtained in solutions containing one of four ALP substrates at bare ITO electrodes. In the cases of AAP and NPP, there were no noticeable currents associated with their oxidation (curves i of Figure 3, parts a and c). The current behavior in Tris buffer (pH 9.6) in the presence of AAP (curve ii of Figure S1 in the Supporting Information) was similar to that in the absence of AAP (curve i of Figure S1 in the Supporting Information). Regarding APP and ANP, the anodic currents were considerable above ca. 0.4 and 0.2 V, respectively (curves i of Figure 3, parts b and d). These results indicate that AAP and NPP are better as an ALP substrate than APP and ANP in terms of both high formal potential and low electrooxidation rate.

Cyclic voltammograms for four ALP products at bare ITO electrodes are shown in curves ii of Figure 3. The reported order of the formal potential is AA and AN < AP < NP.[13] Oxidation currents of AA, AP, and NP were considerable in the given potential ranges (curves ii of Figure 3a−c). Interestingly, the anodic currents of AN were not observed (curve ii of Figure 3d), due to the rapid oxidation of AN by the dissolved oxygen.[23] Consequently, AA is better as an ALP product than other ALP products in terms of both low formal potential and fast electrooxidation rate.

Cyclic voltammograms obtained in the presence of both ALP product and TCEP are shown in curves iii of Figure 3. Oxidation currents of AA in the presence of TCEP (curve iii of Figure 3a) were higher in a wide range of potentials than in the absence of TCEP (curve ii of Figure 3a). In the presence of TCEP (in fact TCEP·HCl), the onset potential appeared at higher potentials because the solution pH was lower than the pH in the absence of TCEP (pH 9.6). In all other cases, oxidation currents were also higher in the presence of TCEP (curves iii of Figure 3b−d). These results indicate that the redox cycling by TCEP increases oxidation currents. Interestingly, oxidation currents of AN were very high in the presence of TCEP (curve iii of Figure 3d), although they were negligible in the absence of TCEP (curve ii of Figure 3d). The reason for this is that AN is entirely oxidized by the dissolved oxygen in the absence of TCEP, whereas AN is generated via reduction of the oxidized AN by TCEP. In the case of AP, the redox cycling allowed very high current increase (curve ii of Figure 3b).

When an electrode is covered with an immunosensing layer, the electrocatalytic activity of the electrode diminishes. To investigate such an influence, the same electrochemical characterization as

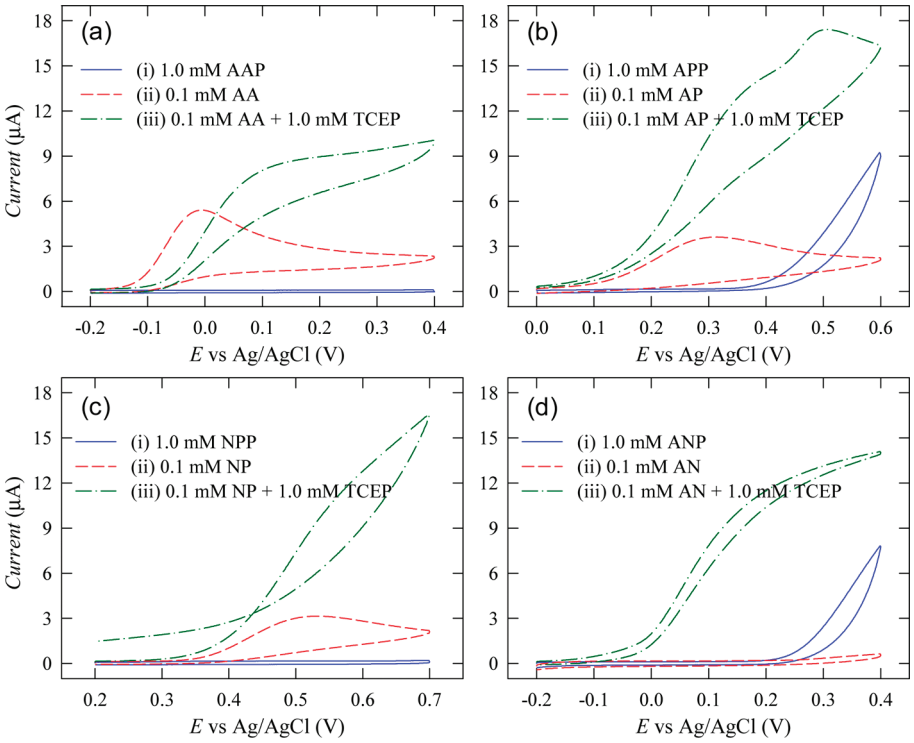

Figure 3. Cyclic voltammograms obtained at bare ITO electrodes (at a scan rate of 20 mV/s) in (i) a Tris buffer solution containing 1.0 mM ALP substrate (pH 9.6), (ii) a Tris buffer solution containing 0.1 mM ALP product (pH 9.6), and a Tris buffer solution containing 0.1 mM ALP product and 1.0 mM TCEP (pH 8.9). ALP substrates are (a) AAP, (b) APP, (c) NPP, and (d) ANP; ALP products are (a) AA, (b) AP, (c) NP, and (d) AN.

that carried out in Figure 3 was performed with avidin-modified ITO electrodes (Figure S2 in the Supporting Information). As for AA, AP, and AN, the avidin modification did not cause any significant change in voltammetric behavior compared to the unmodified case (Figure S2a–d in the Supporting Information and Figure 3, parts a and d). However, the anodic peak of NP at the avidin-modified electrode was shifted to a much higher potential (curve ii of Figure S2c in the Supporting Information), and oxidation currents in the presence of TCEP at the avidin-modified electrode were much smaller (curve iii of Figure S2c in the Supporting Information). Consequently, the avidin modification gives low detrimental effects on electrooxidation of AA, AP, and AN than on electrooxidation of NP.

Overall, AAP is better than other ALP substrates, and AA and AP are better than other ALP products. Moreover, considering (i) easy dissolution of AAP and AA in aqueous solutions, (ii) high formal potential of AAP, and (iii) low formal potential of AA, AAP and AA are better than APP and AP, respectively. As the concentration of TCEP increased, the currents by the redox cycling of AA increased (Figure S3 in the Supporting Information). However, oxidation currents of TCEP also increased with increasing TCEP concentration. A concentration of 2.0 mM was chosen for high signal amplification and low background level.

Conditions for Enzymatic Reaction. The activity of an ALP enzyme depends on the type of buffer, temperature, concentration of $MgCl_2$, and pH of solution. To search for optimum conditions, electrochemical signals for AA were obtained after ALP-conjugated antimouse IgG was immobilized onto ITO electrodes and AAP hydrolysis by the ALP-modified electrode was performed under different conditions (Figure S4a in the Supporting Information). A pH of 9.6 was selected for the pH of the buffer solutions.[7] Judging from Figure S4b–d in the Supporting Information, the enzymatic reaction in the Tris and carbonate buffers was better than in the borate buffer, the reaction at 30 °C was better than at 25 and 35 °C, and the reaction in 10 mM $MgCl_2$ was better than in 0.1 and 1.0 mM $MgCl_2$. These optimum conditions were used for further experiments. It is well-known that ALP activities are inhibited by thiol-containing compounds such as dithiothreitol,[7] which is a commonly employed reducing agent instead of TCEP for breaking disulfide bonds. We found that TCEP did not cause inhibitory effects upon the enzymatic reaction (see the Supporting Information and Figure S5).

Avidin-Modified ITO Electrodes and Nonspecific Binding. In ultrasensitive immunosensors, it is of great importance to minimize nonspecific protein binding, especially ALP-labeled IgGs. In this study, avidin-and-BSA-modified ITO electrodes were used to obtain low nonspecific binding.

Avidin adsorbs well onto solid surfaces because of its carbohydrate content and basic isoelectric point,[7] which may allow a thorough covering of ITO electrodes. Guo and co-workers reported that avidin is passively and stably adsorbed onto ITO electrodes and well covers the surface of the ITO electrodes.[26,27] To examine this effect, the surface concentration of avidin on avidin-modified ITO electrodes was measured. HABA, a dye that binds to avidin, is widely used to quantify biotin and investigate the kinetics of biotin–avidin binding; HABA has an absorbance maximum at a wavelength of 350 nm, whereas the HABA–avidin complex has an absorbance maximum at 500 nm.[7] To date, however, there is no report in which HABA is used to determine the surface concentration of avidin.

Figure 4a illustrates the procedure that we developed to measure the surface concentration of avidin. Avidin was adsorbed onto ITO electrodes in PBS buffer (pH 7.4) or carbonate buffer

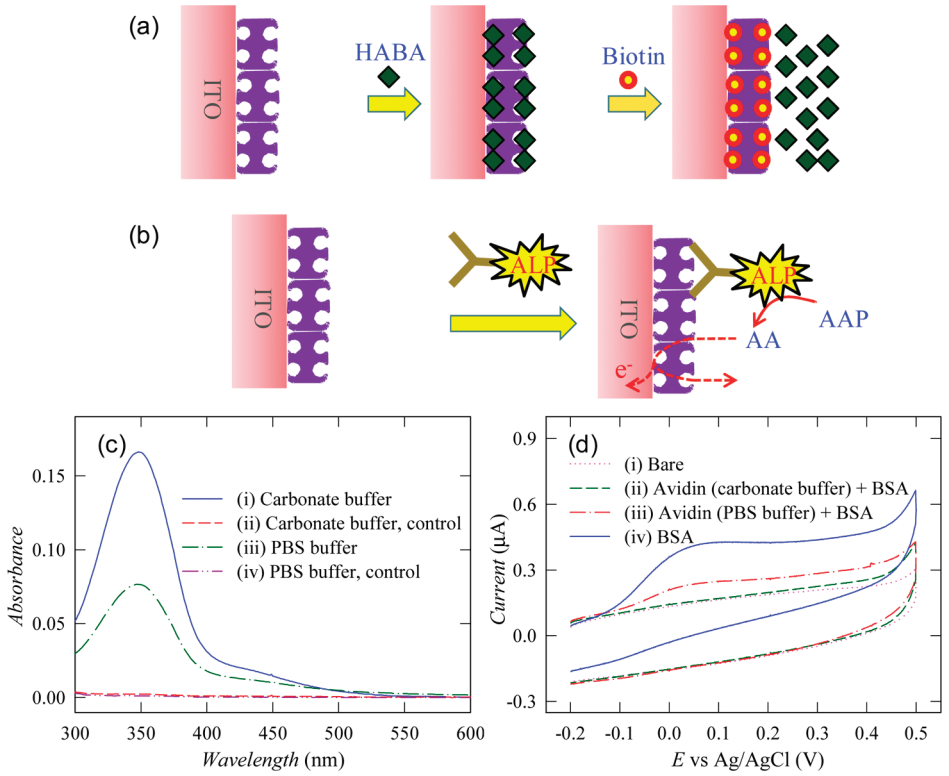

Figure 4. (a) Schematic of the procedure used to measure the surface concentration of avidin. (b) Schematic of the procedure used to measure the level of nonspecific binding of ALP-conjugated antimouse IgG to an avidin-and-BSA-modified ITO electrode. (c) Absorption spectrum obtained after the experiment in panel a was carried out. (d) Cyclic voltammograms obtained in a Tris buffer solution containing 1 mM AAP (pH 9.6) after the experiment in panel b was carried out.

(pH 9.6), and HABA was then bound to all biotin-binding sites of the adsorbed avidin. Afterward, HABA was replaced by biotin. Finally, the concentration of a solution containing the detached HABA was determined by measuring the absorbance at 350 nm. Curve i of Figure 4c shows an absorption spectrum obtained after avidin was adsorbed in carbonate buffer, and curve ii of Figure 4c shows a spectrum obtained as a control experiment, where biotin was bound to the adsorbed avidin prior to the HABA treatment. In this case, HABA cannot bind to the biotin-binding sites of avidin. As biotin does not have absorption at 350 nm, the absorbance at 350 nm is entirely due to the absorption by HABA. The measured extinction coefficient of HABA at 350 nm was 20 700 M^{-1} cm^{-1}. Assuming that four HABAs bind to each avidin, the calculated surface concentration was $9.2 \pm 1.0 \times 10^{-11}$ mol/cm^2, much larger than the theoretical maximum surface concentration of avidin at an avidin monolayer (5.5×10^{-12} mol/cm^2).[28] For comparison, absorption spectra were obtained in the case that avidin was adsorbed in PBS buffer (pH 7.4) (curves iii and iv of Figure 4c). In this case, the calculated surface concentration was $4.4 \pm 0.3 \times 10^{-11}$ mol/cm^2, lower than in the case of the avidin adsorption in carbonate buffer and, interestingly, comparable to the previously reported surface concentration of avidin at avidin-modified ITO electrodes prepared in 20 mM phosphate buffer (pH 7.5) (2.5×10^{-11} mol/cm^2).[26] One of the reasons for the high surface concentrations might be that real surface areas are much larger than geometric surface areas, resulting from high surface roughness of ITO electrodes. The high surface concentrations indicate that avidin well covers the ITO electrodes in carbonate buffer better (pH 9.6).

Next, the levels of nonspecific binding to an avidin-and-BSA-modified ITO electrode and to a BSA-modified ITO electrode were investigated. To achieve this, ALP-conjugated antimouse IgG was nonspecifically adsorbed onto the modified ITO electrodes, the enzymatic reaction proceeded for 10 min in an AAP solution, and cyclic voltammograms were then obtained (Figure 4b). The anodic current behavior obtained with the avidin-and-BSA-modified electrode prepared in carbonate buffer (curve ii of Figure 4d) was similar to that obtained without the enzymatic reaction at a bare ITO electrode (curve i of Figure 4d), indicating the level of nonspecific binding to the avidin-and-BSA-modified ITO electrodes to be very low. The anodic currents obtained with the avidin-and-BSA-modified electrode prepared in PBS buffer (curve iii of Figure 4d) were higher than those in carbonate buffer (curve ii of Figure 4d), indicating a certain level of nonspecific binding on the electrode prepared in PBS buffer. The anodic currents obtained with the BSA-modified ITO electrode (curve iv of Figure 4d) were much larger, implying a much higher level of nonspecific binding to the BSA-modified ITO electrode. These results clearly indicate that the avidin-and-BSA-modified electrodes prepared in carbonate buffer show a very low level of nonspecific binding, along with a higher surface concentration of avidin.

Conditions for Antigen−Antibody Binding. The amount of target protein bound to an immunosensing surface increases with increasing the time of incubation and becomes saturated in a certain time. The time required for saturation increases with decreasing the concentration of target protein. To examine the saturation time, electrochemical signals were obtained in different

dx.doi.org/10.1021/ac200447b |*Anal. Chem.* 2011, 83, 3926–3933

times of incubation (Figure S6a in the Supporting Information). The target solution was dropped onto an immunosensing electrode at room temperature, and the electrode was kept at 4 °C. When a target (mouse IgG) concentration of 1 pg/mL was tested, an incubation time of 30 min was sufficient to obtain saturation (Figure S6a in the Supporting Information). This result suggests that the target binding to an immunosensing surface is fast, even in a low concentration of target at 4 °C.

Highly reproducible data are essential for obtaining ultrasensitive detection. The reproducibility of the sensor response depends highly upon reaction temperature. Accordingly, it is important to maintain optimum temperatures during enzymatic reactions and antigen−antibody bindings. A temperature of 30 °C was selected as the reaction temperature of ALP, according to the results of Figure S4b in the Supporting Information. Room temperature and 37 °C are commonly used for antigen−antibody bindings. A temperature of 4 °C is frequently used to perform an antigen−antibody binding for a long incubation time.[29,30] In this study, antigen−antibody binding was tested at 25 and 4 °C. In sandwich-type immunosensors, two antigen−antibody bindings are required. The first binding occurs between a target and an immunosensing surface, and the second occurs between ALP-conjugated IgG and a target. The electrochemical signals were higher and much more reproducible when both the first and second bindings were carried out at 4 °C than when one of two bindings were carried out at 25 °C (Figures S6b and S7 in the Supporting Information). The antigen−antibody binding at 4 °C was extremely important in obtaining reproducible results, i.e., ultralow detection limits. The concentration of the ALP-conjugated IgG used for the second binding is of great importance in terms of low nonspecific binding and high signal amplification. We found that 10 μg/mL ALP-conjugated IgG was good for low nonspecific binding and high signal amplification (see the Supporting Information).

Immunosensor Performance in the Absence and Presence of Redox Cycling. To evaluate the performance of the presented immunosensing scheme, two target proteins (mouse IgG and troponin I) were tested in the absence and presence of TCEP. Concentration-dependent cyclic voltammograms obtained in the absence of TCEP are shown in Figure S9, parts a and b, in the Supporting Information (for mouse IgG in PBSB buffer) and in Figure 5a and Figure S10 in the Supporting Information (for troponin I in serum). In both cases, the oxidation currents increased with increasing target concentration. The current at 0.035 V at a troponin I concentration of 100 fg/mL ($7.2 \pm 0.5 \times 10^{-7}$ A) were much higher than at a concentration of zero ($3.8 \pm 0.3 \times 10^{-7}$ A) (Figure 5a), and the cyclic voltammograms were highly reproducible (see Figure S11 in the Supporting Information). Figure S9c in the Supporting Information and Figure 5b represent calibration plots for mouse IgG and troponin I, respectively. The estimated detection limits were ca. 10 fg/mL for mouse IgG and ca. 100 fg/mL for troponin I. These ultralow detection limits were possible because oxidation currents at a concentration of zero were low and highly reproducible.

Concentration-dependent cyclic voltammograms obtained in the presence of TCEP are shown in Figure S12, parts a and b, in the Supporting Information (for mouse IgG) and Figure S13, parts a and b, in the Supporting Information (for troponin I). These figures also show that oxidation currents increased with increasing the concentration of target in a wide range of concentrations. The current at 0.2 V at a concentration of 10 fg/mL

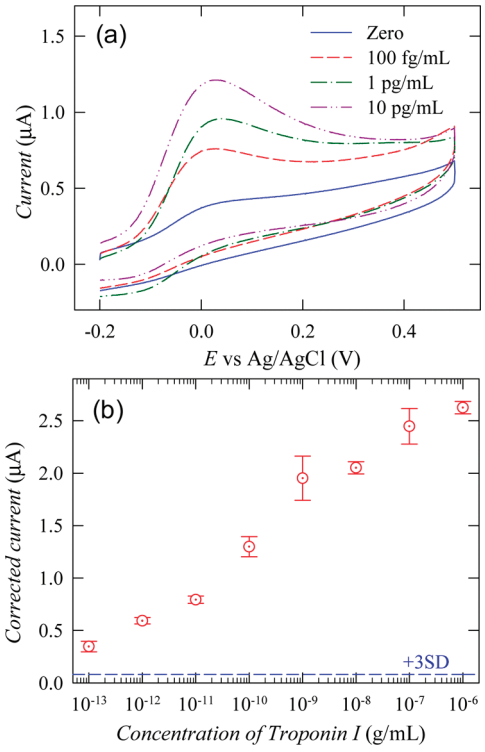

Figure 5. Results of the immunosensing experiments (without redox cycling by TCEP) of Figure 2 that were carried out with human serum containing different concentrations of troponin I. (a) Cyclic voltammograms obtained (at a scan rate of 20 mV/s) in a Tris buffer solution containing 1.0 mM AAP (pH 9.6) after 10 min of incubation. (b) Calibration plot for the detection of troponin I: concentration dependence of the current at 0.035 V in cyclic voltammograms. All data were subtracted by the mean current at a concentration of zero determined by seven measurements. The dashed line corresponds to 3 times the standard deviation (SD) of the current at a concentration of zero. The error bars represent the SD of three measurements.

($1.66 \pm 0.14 \times 10^{-6}$ A) was much higher than at a concentration of zero ($7.1 \pm 0.7 \times 10^{-7}$ A) (Figure S13c in the Supporting Information), and the cyclic voltammograms were highly reproducible (see Figure S14 in the Supporting Information). Figures S12c and S13c in the Supporting Information represent calibration plots for mouse IgG and troponin I, respectively. The estimated detection limits were ca. 1 fg/mL for mouse IgG and ca. 10 fg/mL for troponin I. Considering molecular weight of mouse IgG (150 kDa) and troponin I (24 kDa),[31] the detection limits of mouse IgG and troponin I correspond to ca. 7 and 400 aM, respectively. Approximately one-order-of-magnitude lower detection limits were achieved in both cases with AA redox cycling by TCEP than those without it.

Immunosensor Using Microfabricated Electrodes. When a microfabricated electrode is applied to an immunosensor, the micropatterning of an immunosensing layer is essential and it highly influences reproducibility of the immunosensor. Therefore, it is very important to achieve the micropatterning in a simple and reproducible manner. In this study, after a micropatterned ITO electrode on a glass substrate was prepared (Figure S15a in the Supporting Information), both ITO and glass surface were simultaneously immobilized with avidin and subsequently BSA (Figure S15b in the Supporting Information). This simple surface modification significantly decreases nonspecific binding of

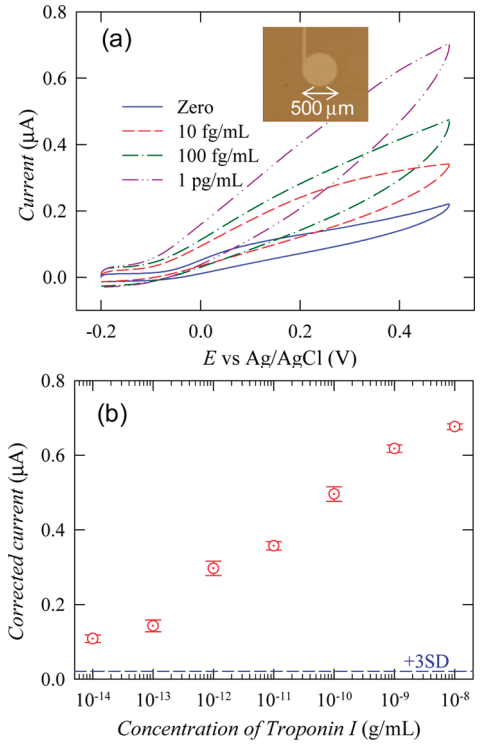

Figure 6. Results of the immunosensing experiments (with redox cycling by TCEP) of Figure 2 that were carried out with microfabricated ITO electrodes with human serum containing different concentrations of troponin I. (a) Cyclic voltammograms obtained (at a scan rate of 20 mV/s) in a Tris buffer solution containing 1.0 mM AAP and 2.0 mM TCEP (pH 8.9) after 10 min of incubation. (b) Calibration plot for the detection of troponin I: concentration dependence of the current at 0.20 V in cyclic voltammograms. The inset in panel a is a microscope image of a micropatterned ITO electrode.

proteins to both ITO and glass surfaces. To immobilize biotinylated antitroponin-I IgG, a solution of biotinylated IgG was dropped over an area larger than the micropatterned disk ITO electrode (diameter = 500 μm, see the inset in Figure 6a). Biotinylated IgG was immobilized on the avidin-modified glass surface near the micropatterned electrode, as well as the avidin-modified ITO electrode. A photograph of a micropatterned ITO electrode is shown in Figure S16a in the Supporting Information. Concentration-dependent cyclic voltammograms obtained in the presence of TCEP are shown in Figure 6a and Figure S16b in the Supporting Information. At a concentration of zero, the currents showed a more rapidly increasing behavior than those in Figure S13a in the Supporting Information, indicating the level of nonspecific binding to be slightly higher. Nevertheless, the detection limit obtained from a calibration plot for troponin I in Figure 6b was also slightly lower than 10 fg/mL, and the data were very reproducible. Importantly, an ultralow detection limit was also achieved with a simply prepared micropatterned immunosensing layer.

CONCLUSIONS

We have developed optimum conditions for a simply prepared and ultrasensitive electrochemical immunosensor using the generation of AA by ALP and the redox cycling of AA by TCEP. The immunosensing surface was prepared by passive avidin adsorption and biotin−avidin conjugation, without the modification with any electrocatalytic material or electron mediator. The ultralow detection limits for troponin I in human serum (ca. 100 fg/mL without the redox cycling and ca. 10 fg/mL with it) come from highly reproducible electrochemical signals, along with high signal amplification and low background level. The simple preparation of the immunosensing surface and the optimization of conditions for enzymatic reaction and antigen−antibody binding enabled us to obtain highly reproducible electrochemical signals. A detection limit of 10 fg/mL was also obtained even when an immunosensing layer was simply formed on a microfabricated ITO electrode. These results suggest that the developed immunosensor could be applied to simply prepared, sensitive, and reproducible immunosensing chips for point-of-care testing. The high stability of TCEP in air and its high solubility in aqueous solutions could enable TCEP to act as an ideal reducing agent (for redox cycling) compatible with immunosensing chips.

ASSOCIATED CONTENT

Supporting Information. More supporting data. This material is available free of charge via the Internet at http://pubs.acs.org.

AUTHOR INFORMATION

Corresponding Author
*E-mail: hyang@pusan.ac.kr.

ACKNOWLEDGMENT

This research was supported by the Public Welfare and Safety Research Program (2010-0020772), the Basic Science Research Program (2009-0085182 and 2009-0072062), and the Nano/Bio Science and Technology Program (2005-01333) through the National Research Foundation of Korea (NRF) funded by the Ministry of Education, Science and Technology.

REFERENCES

(1) Friess, U.; Stark, M. *Anal. Bioanal. Chem.* **2009**, *393*, 1453–1462.
(2) Tate, J. R. *Clin. Chem. Lab. Med.* **2008**, *46*, 1489–1500.
(3) Iwanaga, Y.; Miyazaki, S. *Circ. J.* **2010**, *74*, 1274–1282.
(4) Das, J.; Jo, K.; Lee, J. W.; Yang, H. *Anal. Chem.* **2007**, *79*, 2790–2796.
(5) Nassef, H. M.; Redondo, M. C. B.; Ciclitira, P. J.; Ellis, H. J.; Fragoso, A.; O'Sullivan, C. K. *Anal. Chem.* **2008**, *80*, 9265–9271.
(6) Wilson, M. S.; Rauh, R. D. *Biosens. Bioelectron.* **2004**, *20*, 276–283.
(7) Savage, M. D.; Mattson, G.; Desai, S.; Nielander, G. W.; Morgensen, S.; Conklin, E. J. *Avidin−Biotin Chemistry: A Handbook*, 2nd ed.; Pierce: Rockford, IL, 1994; pp 155−156.
(8) Thomas, J. H.; Kim, S. K.; Hesketh, P. J.; Halsall, H. B.; Heineman, W. R. *Anal. Chem.* **2004**, *76*, 2700–2707.
(9) Elsholz, B.; Wörl, R.; Blohm, L.; Albers, J.; Feucht, H.; Grunwald, T.; Jürgen, B.; Schweder, T.; Hintsche, R. *Anal. Chem.* **2006**, *78*, 4794–4802.
(10) Kwon, S. J.; Yang, H.; Jo, K.; Kwak, J. *Analyst* **2008**, *133*, 1599–1604.
(11) Wilson, M. S.; Nie, W. *Anal. Chem.* **2006**, *78*, 2507–2513.
(12) Dong, H.; Li, C. M.; Zhang, Y. F.; Cao, X. D.; Gan, Y. *Lab Chip* **2007**, *7*, 1752–1758.
(13) Preechaworapun, A.; Dai, Z.; Xiang, Y.; Chailapakul, O.; Wang, J. *Talanta* **2008**, *76*, 424–431.

(14) Bauer, C. G.; Eremenko, A. V.; Ehrentreich-Förster, E.; Bier, F. F.; Makower, A.; Halsall, H. B.; Heineman, W. R.; Scheller, F. W. *Anal. Chem.* **1996**, *68*, 2453–2458.
(15) Aziz, M. A.; Patra, S.; Yang, H. *Chem. Commun.* **2008**, *38*, 4607–4609.
(16) Moore, E. J.; Pravda, M.; Kreuzer, M. P.; Guilbault, G. G. *Anal. Lett.* **2003**, *36*, 303–315.
(17) Tsukatani, T.; Ide, S.; Ono, M.; Matsumoto, K. *Talanta* **2007**, *73*, 471–475.
(18) Kokado, A.; Arakawa, H.; Maeda, M. *Anal. Chim. Acta* **2000**, *407*, 119–125.
(19) Hansen, R. E.; Winther, J. R. *Anal. Biochem.* **2009**, *394*, 147–158.
(20) Lykkesfeldt, J. *Anal. Biochem.* **2000**, *282*, 89–93.
(21) Bova, M. P.; Mattson, M. N.; Vasile, S.; Tam, D.; Holsinger, L.; Bremer, M.; Hui, T.; McMohan, G.; Rice, A.; Fukuto, J. M. *Arch. Biochem. Biophys.* **2004**, *429*, 30–41.
(22) Nath, N.; Hyun, J.; Ma, H.; Chilkoti, A. *Surf. Sci.* **2004**, *570*, 98–110.
(23) Másson, M.; Rúnarsson, Ö. V.; Jóhannson, F.; Aizawa, M. *Talanta* **2004**, *64*, 174–180.
(24) Kim, B. K.; Yang, S. Y.; Aziz, M. A.; Jo, K.; Sung, D.; Jon, S.; Woo, H. Y.; Yang, H. *Electroanalysis* **2010**, *22*, 2235–2244.
(25) Zudans, I.; Paddock, J. R.; Kuramitz, H.; Maghasi, A. T.; Wansapura, C. M.; Conklin, S. D.; Kaval, N.; Shtoyko, T.; Monk, D. J.; Bryan, S. A.; Hubler, T. L.; Richardson, J. N.; Seliskar, C. J.; Heineman, W. R. *J. Electroanal. Chem.* **2004**, *565*, 311–320.
(26) Guo, L. H.; Yang, X. Q. *Analyst* **2005**, *130*, 1027–1031.
(27) Wei, M. Y.; Guo, L. H.; Chen, H. *Microchim. Acta* **2006**, *155*, 409–414.
(28) Frey, B. L.; Jordan, C. E.; Komguth, S.; Com, R. M. *Anal. Chem.* **1995**, *67*, 4452–4457.
(29) Key, M., Ed. *Immunohistochemical Staining Methods*, 4th ed.; Dako: Carpinteria, CA, 1996; pp 18.
(30) Lockshin, M. D.; Qamar, T.; Levy, R. A.; Best, M. P. *J. Clin. Immunol.* **1988**, *8*, 188–192.
(31) Bodor, G. S.; Porter, S.; Landt, Y.; Ladenson, J. H. *Clin. Chem.* **1992**, *38*, 2203–2214.